

# UC Davis

## Recent Work

### Title

Heat Transfer Limitations in Hydrogen Production Via Steam Reformation: The Effect of Reactor Geometry

### Permalink

<https://escholarship.org/uc/item/6sv8j32g>

### Authors

Vernon, David R.  
Davieau, David D.  
Dudgeon, Bryce A.  
et al.

### Publication Date

2006-06-01

Peer reviewed

## FUELCELL2006-97109

### HEAT TRANSFER LIMITATIONS IN HYDROGEN PRODUCTION VIA STEAM REFORMATION: THE EFFECT OF REACTOR GEOMETRY

David, R., Vernon

David, D., Davieau

Bryce, A., Dudgeon

Paul, A., Erickson

University of California Davis,  
 Mechanical and Aeronautical Engineering Department,  
 Hydrogen Production and Utilization Laboratory

#### ABSTRACT

Hydrogen can be produced in a variety of methods including steam-reformation of hydrocarbon fuels. In past studies the quasi non-dimensional space velocity parameter (inverse residence time) has been shown to be insufficient in accurately predicting fuel conversion in hydrocarbon-steam reformation. Heat transfer limitations have been manifest with reactors of different geometries. In order to achieve ideal fuel conversion, the heat transfer limitations and the changes of these limitations with respect to geometry must be considered in the reactor design. In this investigation, axial and radial temperature profiles are presented from reactors of different aspect ratios while holding space velocity constant. Using both the temperature profile information as well as the traditional space velocity limitations one may be able to develop an optimal reactor design.

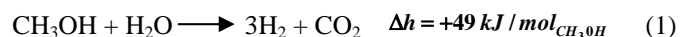
#### NOMENCLATURE

A	Arrhenius pre-exponential constant
Ea	Arrhenius activation energy
k	Reaction rate constant
MLHSV	Methanol Liquid Hourly Space Velocity
X	Methanol conversion
[i]	Molar concentration of species i
[i] <sub>inlet</sub>	Molar concentration of species i at the inlet
[i] <sub>outlet</sub>	Molar concentration of species i at the outlet

#### INTRODUCTION

Reformation of hydrocarbon feed stocks can supply hydrogen for many uses including transportation fuel. Steam reformation of methanol can produce hydrogen in concentrations greater than 60% at temperatures between 225°C and 290°C [1]. The low temperature requirements and

high hydrogen concentration produced make methanol a very interesting option for supplying hydrogen in distributed or on-board applications for vehicles. Steam reformation of methanol is an endothermic chemical reaction which takes place in packed bed reactors and requires external heating. The ideal methanol reformation reaction produces only H<sub>2</sub> and CO<sub>2</sub> in the catalyst bed. The ideal reaction is characterized by equation (1).



The rate of this reaction can be modeled by a simple bi-molecular rate law, shown in equation (2). In this model the rate constant, k, follows an exponential dependence on temperature based on the Arrhenius rate law, equation (3). The pre-exponential term A and the activation energy, Ea, depend upon the catalyst used. The reaction proceeds more quickly at higher temperatures.

$$\frac{d[\text{CH}_3\text{OH}]}{dt} = -k[\text{H}_2\text{O}][\text{CH}_3\text{OH}] \quad (2)$$

$$k = Ae^{-Ea/RT} \quad (3)$$

More complex rate laws relating competition of molecular species for heterogeneous catalyst sites in a detailed reaction mechanism can be developed to model steam reformation reactions. These more complex reaction rate models still incorporate Arrhenius based rate constants so the following discussion of the effects of temperature are still

applicable and this simple case is illustrative of the general phenomenology.

One important metric for measuring the performance of a steam reforming reactor is called conversion. The conversion is defined in the equation (4) below.

$$X = \frac{[CH_3OH]_{inlet} - [CH_3OH]_{outlet}}{[CH_3OH]_{inlet}} \times 100\% \quad (4)$$

For design of reactors the quasi non-dimensional parameter space velocity, inverse residence time, has been used to predict conversion for reactors of different geometries. In methanol reformation the metric of comparison is the Methanol Liquid Hourly Space Velocity (MLHSV), which is defined in the equation below.

$$MLHSV = \left( \frac{\frac{m^3}{hr} \text{ liquid methanol input}}{m^3 \text{ reactor volume}} \right) \quad (5)$$

As presented by Davieau a reactor will show decreased conversion at higher flow rates, higher space velocities, since residence time decreases [2]. The general behavior of this decrease in conversion is illustrated in figure #1 below.

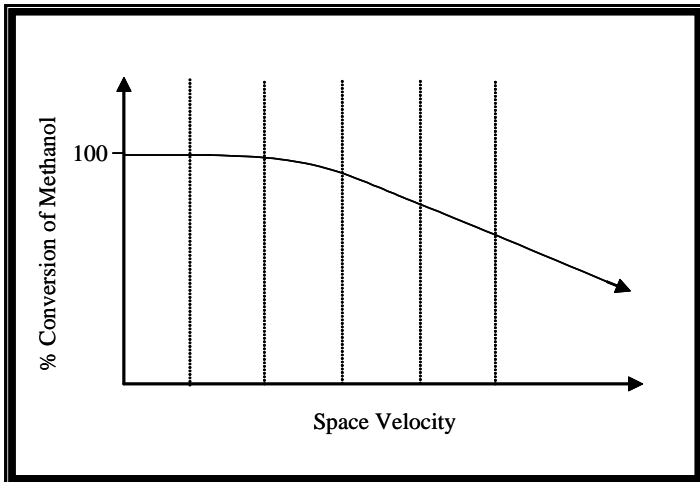


Figure #1 General conversion versus space velocity [2]

Previous work measuring the effects of reactor temperature on conversion has used space velocity to define

reactor characteristics without specifying reactor geometry [3]. Recent work has shown that space velocity alone is an insufficient parameter for predicting conversion for reactors of different geometries [2,4,5,6]. In conjunction with space velocity, both heat and mass transfer limitations play important roles in determining the actual conversion achieved by a specific reactor design. Real reactor designs deviate significantly from the isothermal plug flow reactor assumptions therefore real reactors experience heat and mass transfer limitations that affect the rate of the reformation reactions. These heat and mass transfer limitations are dependant on reactor geometry and therefore the reformation reaction rate is also dependant on reactor geometry. The variation in heat transfer limitations with geometry can be examined by measuring the temperature profiles in reactors of different geometries at the same space velocity with the same heating control algorithms.

Temperature profile measurements allow the comparison of active zones in reactors of different geometries. When comparing profiles regions of low temperature reside near the entrance of the reactor where the endothermic reaction has consumed the heat energy carried by the reactants at the inlet temperature and where the reactant concentrations are still high enough to make heat transfer into this area the limiting step in the reformation process. The position and length of this cooler active zone provides insight into the relative performance of different reactor geometries.

For practical commercial applications it is important to reduce the complexity of the reformer systems. Laboratory scale sensing and control systems are too complex and costly for use in commercial applications. A major goal in reformer development is to reduce the number of sensors required to control a reactor. Knowledge of the relationship between temperatures at one point in the reactor and that of the other points allow fewer measurements to provide much more information about the operating conditions and appropriate control inputs. The study of the temperature profiles allows optimal selection of control sensor positions.

Previous work has measured temperature profiles in steam reformation reactors noting space velocity without fully specifying reactor geometry [3,9]. A number of studies have modeled the temperature profile in steam reformation reactors [10,11] some of these have performed temperature measurements in order to calibrate the models or compare model results to empirical results [10]. Often temperature measurements have been performed only near the wall and at the centerline of the reactor [2,5,6,8,10]. More ambitious projects have measured the radial temperature profile at several points radially across one half of the reactor at several points along the longitudinal axis [4].

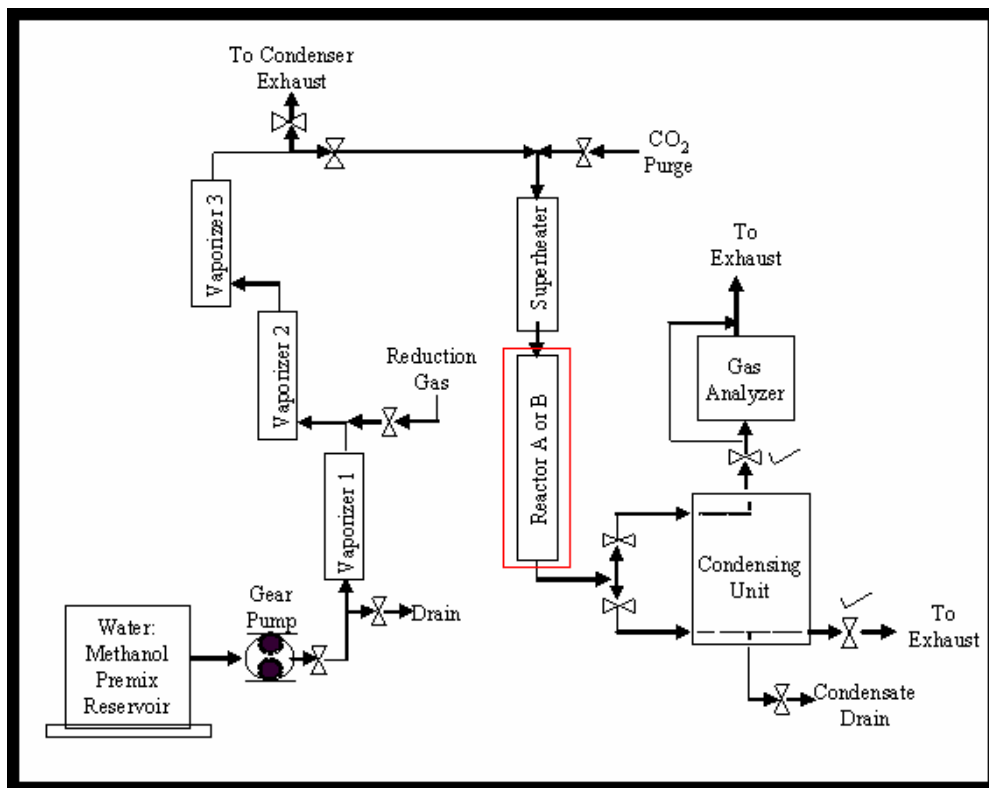


Figure 2: Schematic of HYPALU reformer/reactor system [2]

In this paper we present temperature measurement data showing the difference in thermal profiles for tubular steam reformation reactors of the same volume with two different aspect ratios operating at the same space velocity. These temperature profiles are based upon temperature measurements across the full reactor diameter at several axial positions. The difference in conversion achieved by the two different reactors is also presented.

## FACILITIES

The reformer system consists of a water and methanol vapor delivery system, the reactor, and a gas analysis system. A digital gear pump is used to meter a precise flow of premixed methanol and water to a vaporizer train. After the vaporizer the gases enter a superheater where they are heated to the desired inlet temperature. The reactors presented in this paper are tubular packed bed reactors with the same internal packed bed volume but with different aspect ratios. The gas analysis system is comprised of a condenser to remove excess water and any unconverted methanol and then gas analyzer to measure the concentrations of gases in the effluent. Figure #1 shows a schematic of the reformer system.

A mixture of 1:1.5 methanol and water based upon weight is used as the premix solution. The premix is pumped through the digital gear pump (Cole-Parmer EW-07002-25) at the flow rate required to achieve a given Gas Hourly Space Velocity (GHSV). The weight of the premix carboy is monitored to precisely measure the flow rate. The premix is then vaporized at 250 °C in the vaporizer section.

The superheater section reduces temperature fluctuations from the vaporizer train and enhances mixing. The vaporized premix enters the packed bed reactor at a temperature of 260°C.

Two different reactors with different geometries are compared in this study. The low aspect ratio reactor has a body 10”(254mm) in length with a 1.378”(35.00mm) ID (1.65” OD, 1-1/4” nominal, schedule 40), whereas the high aspect ratio reactor has a body 24”(609.6mm) in length with a 0.791”(20.09mm) ID (1.05” OD, ¾” nominal, schedule 40). Both reactors are made from commercially available 316 stainless steel tube. Thermocouples enter the reactor from the left hand side through the evenly spaced thermocouple ports. For the high aspect ratio reactor the thermocouple ports are spaced 2.65” (67.4mm) apart. For the low aspect ratio reactor the thermocouple ports are spaced 2.0”(50.5mm) apart.

The catalyst used in these experiments is Copper / Zinc Oxide pelletized catalyst part number FCRM-2 commercially available from Sud-Chemie.

To supply the heat required to drive the endothermic reformation reaction the packed bed reactor is externally heated with electric band heaters, see Figure #3 and Figure #4. A surface thermocouple is placed underneath each band heater to measure the outer surface temperature of the reactor tube. A set of temperature control algorithms in LabVIEW is used to control the heaters according to the temperature readings from the outer surface of the reactor.

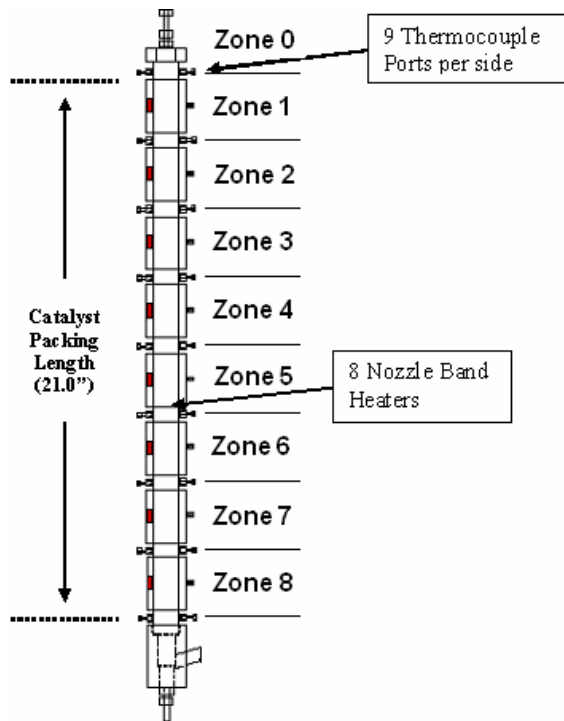


Figure 3: Schematic of High Aspect Ratio packed bed reactor

analyzer (NOVA Analytical Systems Inc. 7904CM), which uses both a thermal conductivity detector and an Infra-Red adsorption detector to measure Hydrogen, CO<sub>2</sub>, CO and Hydrocarbon concentrations.

Special thermocouples were designed and fabricated in-house to substantially reduce the effects from sheath conduction and more accurately measure the true gas temperature inside the reactor. These special thermocouples use Miniature, K-type, 304 SST Sheath, 0.020" diameter, 12" length, ungrounded OMEGA thermocouples with an insulated support to reduce probe thermal conductivity errors. A comparison of measurements made with different types of thermocouples has been performed but is beyond the scope of this paper and will be discussed in future publications. Exterior thermocouples are placed directly between the heater bands and the reactor tube wall to measure the surface temperature of the reactor. These exterior surface thermocouples are Miniature, K-type, 304 SST Sheath, 0.010" diameter, 12" length, ungrounded OMEGA thermocouples. All of the data acquisition is performed using National instruments hardware.

To control the volume of the packed bed the catalyst loading process uses a specified weight of catalyst, which is loaded into the reactor tubes on top of a bottom supporting screen to hold the bottom position of the catalyst bed above the last thermocouple port. See Figure #2 and Figure #3 for a schematic diagram showing where the catalyst bed lies within each reactor. The distance of the catalyst from the top of the reactor is measured giving the total catalyst bed height. The volume of the catalyst bed is calculated from the catalyst bed height and the ID of the reactor. The catalyst bed within the high aspect ratio reactor is 21.01" (533.7mm) long, giving an aspect ratio of 26.56. The catalyst bed within the low aspect ratio reactor is 7.45" (189.3mm) long, giving an aspect ratio of 5.41. The total volume of the catalyst bed for the High aspect ratio reactor it is 0.169 L. The total volume of the catalyst bed for the Low aspect ratio reactor is 0.182 L.

After loading into the reactors the catalyst is reduced at 190°C using 2.0% hydrogen in nitrogen until the hydrogen concentration in the effluent reaches 2.0%, requiring an average of approximately 10 hours.

## EXPERIMENTAL

Measurement of the radial and axial temperature profile was accomplished by first positioning all of the thermocouples entering from the left hand side of the reactor so that they extend all the way across the diameter of the reactor with the tips at the far wall (right hand wall). The reformer reactor system was allowed to stabilize at a particular set of operating conditions for at least ten minutes using the right hand side inside wall thermocouples as control signals for the heaters. After stabilizing, data was recorded for ten minutes to calculate the average external wall temperatures. The average external wall temperatures were then used as control set points for the heater bands using the external wall thermocouples as the

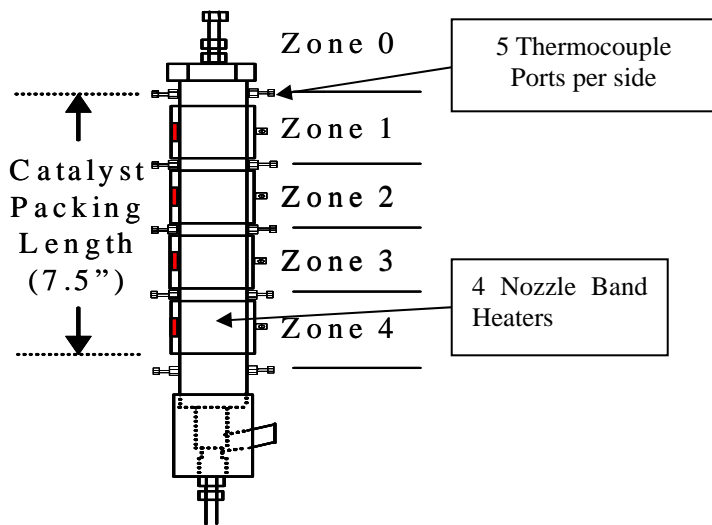


Figure 4: Schematic of Low Aspect Ratio packed bed reactor

The effluent product gas stream exits the reactor and is then sent to the condenser where excess water and any unconverted methanol is condensed and analyzed to determine conversion. The remaining product gases pass to the gas

control sensors and the reactor was allowed to operate at steady state for at least 5 minutes.

At each measurement position data is recorded for approximately five minutes, which yields 195 data points. After the data is collected for the first radial position (right hand wall) the left hand side thermocouples are traversed towards the left hand side of the reactor by 2.5mm. After completing the traverse the system was allowed to stabilize for at least 5 minutes before the next set of data were recorded. These steps were repeated at all axial zones for each radial position until all of the left hand side thermocouples reach the left hand side wall. For the high aspect ratio reactor there were 9 traverse steps with 7 thermocouples. For the low aspect ratio reactor there were 15 traverse steps with 3 thermocouples. In this way the radial temperature profile was measured across the full diameter of the reactor at each axial (zone) position along the length of the reactor.

## RESULTS AND DISCUSSION

As described above the radial temperature profiles were measured for two reactors of the same internal volume but different aspect ratios with the same reactant flow rates. The temperature data were used to generate visualizations using two dimensional biaxial interpolations between the measured points to give the profile in both the radial and axial directions.

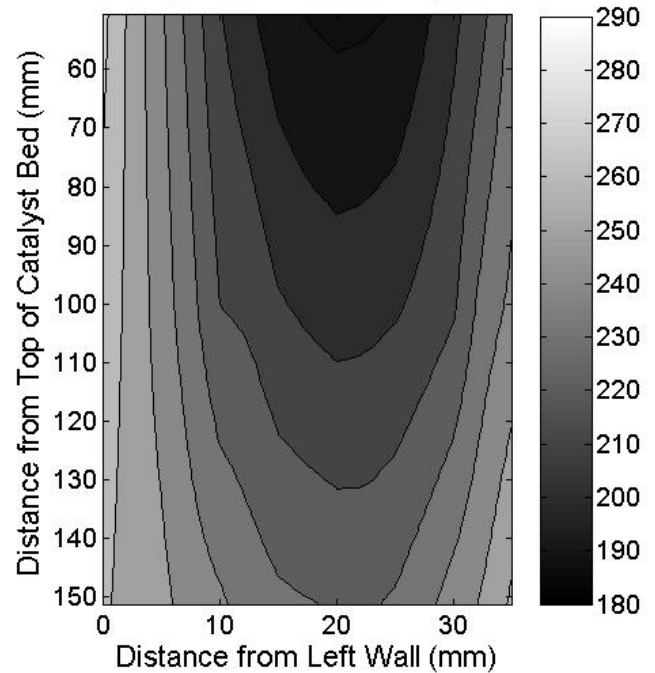
The temperature profiles are shown in figures #5-8 below. Error bars using a 95% confidence interval for the temperature measurements and for the position of the probe tips show negligible changes in the temperature data. The largest sample average standard deviation of any single measurement was 0.33°C, giving a large sample 95% confidence interval of +/- 0.66°C. The maximum total 95% confidence interval uncertainty in any temperature measurement was +/-2.39°C, with the +/-2.2°C wire bias uncertainty from the thermocouples being the major source of uncertainty.

The minimum average temperature over the five minute data collection period is significantly lower in the low aspect ratio reactor than in the high aspect ratio reactor, as summarized in table #1 for both the low 5ml/min flow rate corresponding to MLHSV 1, and for the high 20ml/min flow rate corresponding to MLHSV 4.

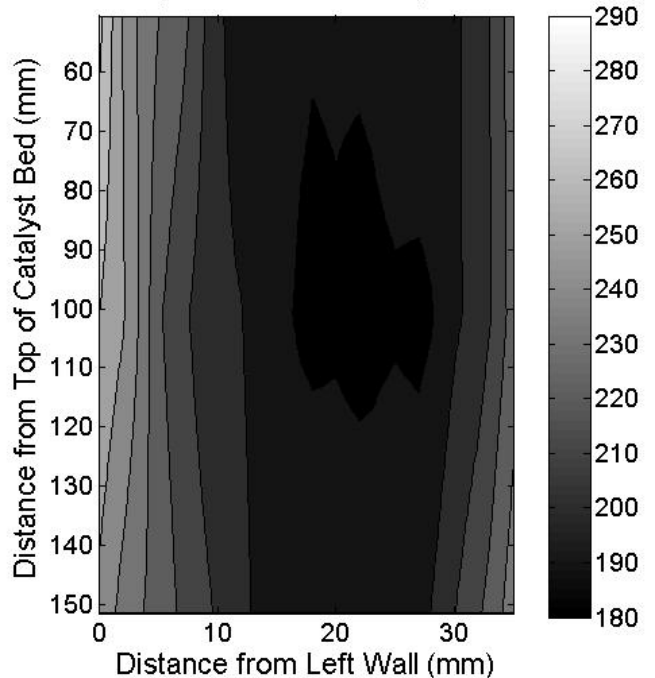
Reactor Aspect Ratio	MLHSV 1		MLHSV 4	
	Min Temp °C	Max Temp °C	Min Temp °C	Max Temp °C
Low	187.6	272.9	186.9	273.0
High	219	289.8	221.1	269.8

Table #1 Minimum and maximum measured gas temperatures

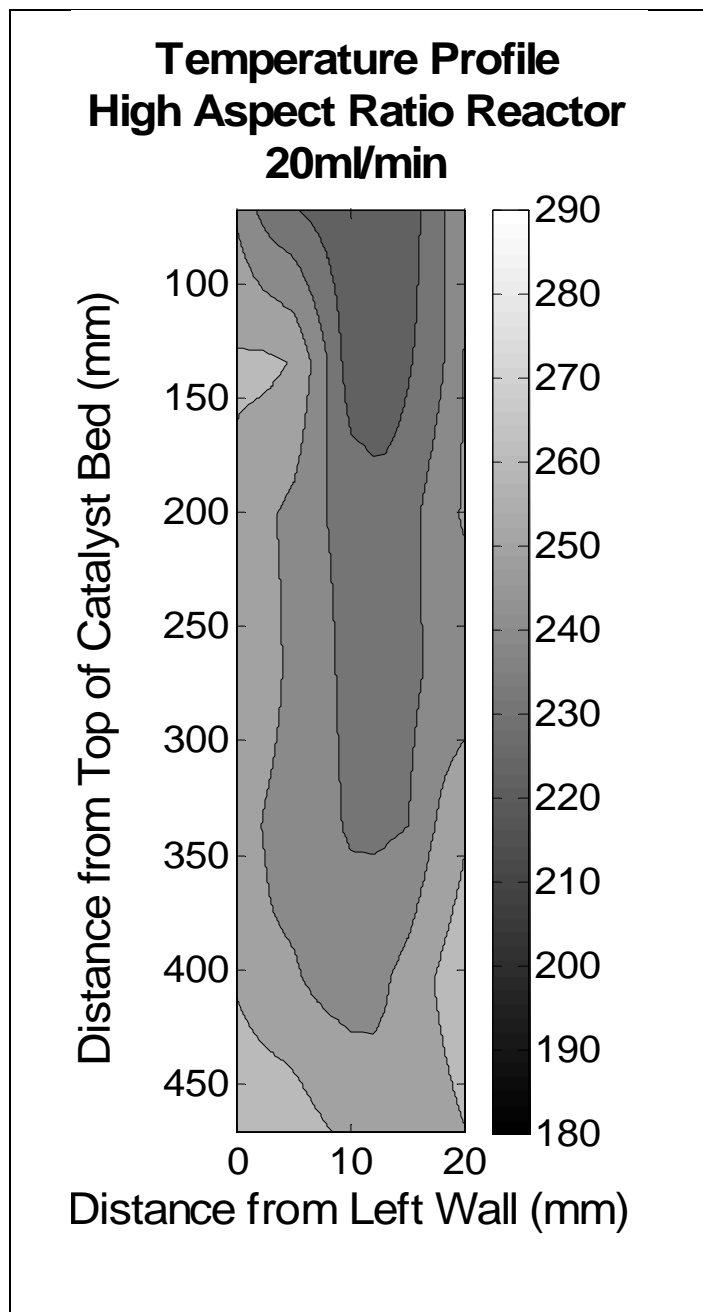
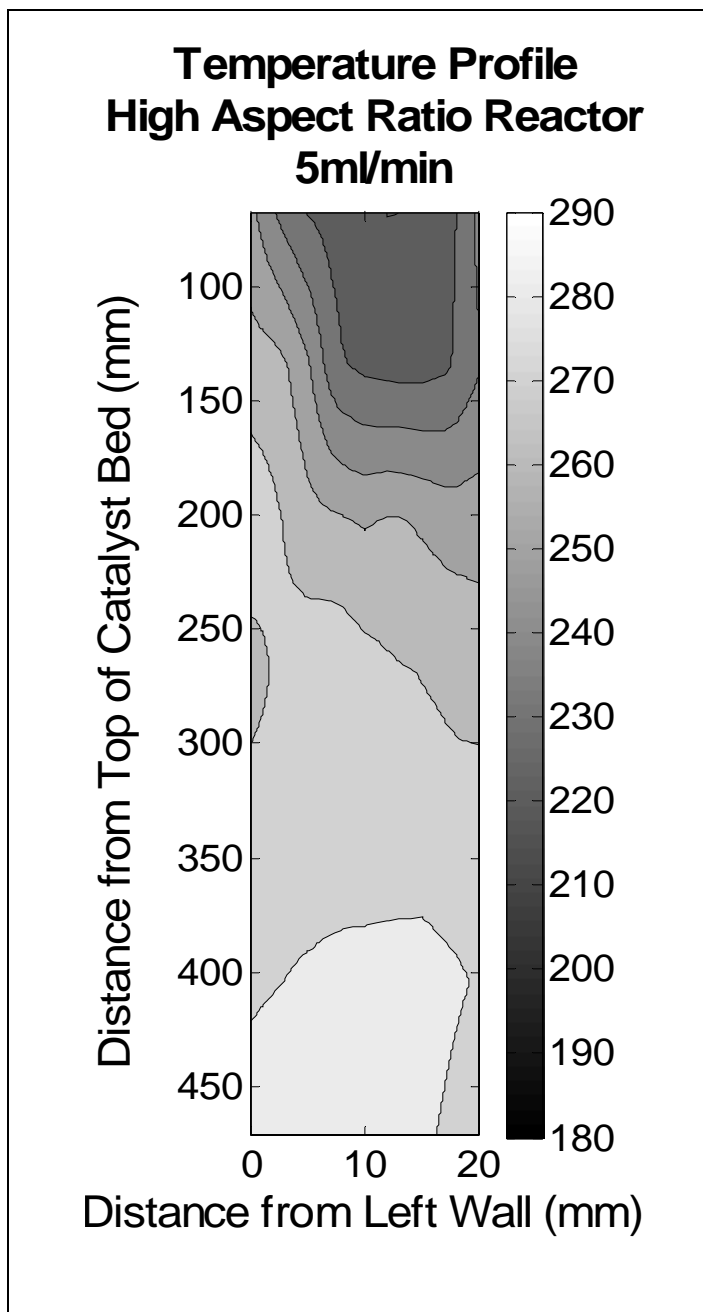
Temperature Profile  
Low Aspect Ratio Reactor, 5ml/min



Temperature Profile  
Low Aspect Ratio Reactor, 20ml/min



Figures #4-5 Radial temperature profile charts for the Low Aspect ratio Reactor at 5 and 20 ml per minute flow rates (corresponding to a GHSV of 1 and 4 respectively)



**Figures #7-8 Radial temperature profile charts for the High Aspect ratio Reactor at 5 and 20 ml per minute flow rates (corresponding to a GHSV of 1 and 4 respectively)**

Note: Comparing the two sets of reactor charts, the temperature colors are on the same scale, the radial distances are on approximately the same scale, Axial scales are different.

It can be seen that the low aspect ratio reactor experiences a larger radial temperature gradient between the wall and the center line than the high aspect ratio reactor, as summarized in table #2. The maximum radial temperature gradient between measurements 2.5mm apart is summarized in table #3.

Reactor Aspect Ratio	MLHSV 1	MLHSV 4
	Max temp difference Inside wall to Center Line °C	Max temp difference Inside wall to Center Line °C
Low	43.6	40.3
High	20.0	27.5

**Table #2 Maximum temperature difference between the inside wall measurement at the far wall of the reactor and the centerline temperature measurement.**

Reactor Aspect Ratio	MLHSV 1	MLHSV 4
	Max temp gradient Inside wall to Center Line °C / cm	Max temp gradient Inside wall to Center Line °C / cm
Low	12.5	11.5
High	10.0	13.7

**Table #3 Maximum temperature gradient between the inside wall measurement at the far wall of the reactor and the centerline temperature measurement.**

The maximum temperature gradient between any two radial positions is summarized in table #4.

Reactor Aspect Ratio	MLHSV 1	MLHSV 4
	Max temp gradient one step °C / 2.5mm	Max temp gradient one step °C / 2.5mm
Low	16.5	29.3
High	20.1	19.9

**Table #4 Maximum radial temperature gradient across for one step of 2.5mm.**

The temperature profiles show a cooler region at the axial position after the heat of the vapor entering the reactor has been consumed by the reaction and there is still significant endothermic reaction taking place. Differences in the position of this cooler region between the low aspect ratio reactor and the high aspect ratio reactors are expected due to the different volumes of catalyst for a given length down the axis of the

reactor as well as the different radial temperature profiles in these top portions of the two reactors.

It is clear that a larger volume of catalyst in the low aspect ratio reactor is at lower temperatures compared to the high aspect ratio reactor. This indicates that there is a more severe heat transfer limitation for the low aspect ratio reactor than for the high aspect ratio reactor. This difference in average temperature may also explain the difference in conversion between the two reactors at the same space velocity.

Table #5 summarizes the conversion data for these two different reactors. As space velocity increases the conversion for the wider low aspect ratio reactor decreases much faster than that of the thinner high aspect ratio reactor.

Reactor Aspect Ratio	Conversion at Space Velocity		
	1	2	4
Low	98.8%	91.0%	66.1%
High	98.7%	96.9%	78.2%

**Table #5 Conversion Data Table**

The phenomenology behind the differences in temperature profiles between the wider low aspect ratio reactor and the thinner high aspect ratio reactor is intuitively apparent. The heat transfer path from the external band heaters to the centerline of the low aspect ratio reactor is significantly longer (1.74 times longer) than that for the thinner high aspect ratio reactor.

It was expected that the temperature profiles for both reactors would be radially symmetric. From the temperature profiles above there is a distinct asymmetry with higher temperatures extending further into the reactor from the left hand side and cooler temperatures reaching further towards the right hand side. This asymmetry was more pronounced when using standard 1/16" thermocouples. We believe that this shift in the temperature profile is caused by the conduction of heat down the thermocouple probe, which biases the temperature measurement away from the true gas temperature. This phenomenon is known as sheath conduction. A full treatment of this issue as well as further details on the design and fabrication of the low probe conductivity thermocouples will follow in a future publication.

## CONCLUSIONS

Clearly reactor geometry affects the heat transfer distance from a heat source into the catalyst bed. Longer heat transfer distances cause more severe limitations to the heat transfer rate. Heat transfer limitations cause temperature gradients along the heat transfer path leading to a temperature profile within the catalyst bed. Since chemical reaction rates change exponentially with temperature these temperature profiles affect the average reaction rate. The total conversion achieved



in a reactor is the spatial integration of the reaction rate over the residence time in the reactor. Therefore conversion at a given space velocity depends upon reactor geometry. In this way different reactor geometries will achieve different total conversions at the same space velocity. Therefore space velocity is an insufficient parameter for predicting conversion.

Both space velocity and temperature profile must be known in order to accurately predict conversion for different reactor designs. Further work in predicting temperature profiles from reactor geometry may enable further optimization of reformer designs.

Current research in the Hydrogen Production and Utilization laboratory is focusing on further investigations of the affects of reactor geometry as well as both active and passive heat and mass transfer enhancements.

## ACKNOWLEDGMENTS

We would like to thank the researchers at the UC Davis Hydrogen Production and Utilization Laboratory for supporting this work. This research project was funded by the U.S. Dept of Energy under DOE Grant Number DE-PS26-02NT41613-06.

## REFERENCES

[1] Brown, Lee F., "A comparative study of fuels for on-board hydrogen production for fuel-cell powered Automobiles", International Journal of Hydrogen Energy, Vol. 26, (2001), pgs. 381-397

[2] Davieau, David D., *An Analysis of Space Velocity and Aspect Ratio Parameters in Steam-Reforming Hydrogen production Reactors*, M.S. Thesis, University of California Davis (2004).

[3] Takeda, K., Baba, A., Hishinuma, Y. and Chikahisa, T., "Performance of a Methanol Reforming System for a Fuel Cell Powered Vehicle and System Evaluation of a PEFC System," Society of Automotive Engineers of Japan, v 23, (2002).

[4] Erickson, Paul A., *Enhancing the Steam-Reforming Process with Acoustics: An Investigation for Fuel Cell Vehicle Applications*, Ph.D. Dissertation, University of Florida, (2002).

[5] Erickson, Paul A., Davieau, David D., Kamisky, Robert J., Zoller, Zachary, "Space Velocity as an Insufficient Parameter in the Steam-Reforming Process," Proceedings of the Seventh IASTED International Conference, Power and Energy Systems, Nov 28 - Dec 1, (2004) Clearwater Beach FL, USA, pgs. 141-145

[6] Erickson, Paul A., Davieau, David D., Kamisky, Robert J., Zoller, Zachary, "Space Velocity as an Insufficient Parameter in the Steam-Reforming Process," International Journal of Power and Energy Systems, Accepted Feb 2005 In Press

[7] Sterchi J. P., *The Effect of Hydrocarbon Impurities on the Methanol Steam-Reforming Process for Fuel Cell Applications*, Ph.D. Dissertation, University of Florida: Gainesville, (2001).

[8] Nagano, Susumu, Miyagawa, Hiroshi, Azegami, Osamu, Ohsawa, Katsuyuki, "Heat Transfer Enhancement in Methanol Steam Reforming for a Fuel Cell", Energy Conversion Management, vol. 42, (2001), pgs. 1817-1829

[9] Wilde, P.J., Verhaak, M.J.F.M. "Catalytic Production of Hydrogen From Methanol", Catalysis Today, Vol. 60, (2000), pgs. 3-10

[10] Usami, Fukusako, Yamada, "Heat and Mass Transfer in a Reforming Catalyst Bed: Analytical Prediction of Distribution sin the Catalyst Bed", Heat Transfer-Asian Research, Vol. 32, (2003)

[11] Boettner, Dasie D., Paganelli, Gino., Guenzenec, Yann G., Rizzoni, Giorgio, Moran, Michael J., "On-Board Reforming Effects on the Performance of Proton Exchange Membrane (PEM) Fuel Cell vehicles.", Journal of Energy Resources Technology, Vol. 124, September (2004), pgs. 191-196